

HEAT TRANSFER IN AIRLIFT REACTORS

P. K. OUYOUNG, M. Y. CHISTI and M. MOO-YOUNG

Department of Chemical Engineering, University of Waterloo, Waterloo, Ontario, Canada

The influence of gas throughput as the principal operating parameter, and of downcomer-to-riser cross-sectional area ratio, on local and global heat transfer coefficients in concentric draught tube airlift devices is reported.

Heating surface-to-fluid heat transfer coefficients are theoretically and experimentally shown to increase with gas velocity raised to 1/4 power. Depending on the flow conditions, the heat transfer rates were either positively or negatively influenced by the presence of cellulose fibre solids in aqueous suspensions used to simulate mycelial fermentation systems.

Airlift vessels were found to produce higher heat transfer coefficients than bubble columns under otherwise identical conditions. Within an airlift device the riser was shown to be the best possible location for heating/cooling surfaces.

INTRODUCTION

For most productive fermentations typical metabolic heat generation¹ is of the order of 3 to 15 kWm⁻³. Higher heat loads occur when highly reduced substrates such as hydrocarbons, are oxidized. Removal of heat can be difficult particularly in large bioreactors, and for satisfactory reactor design a knowledge of heat transport in these devices is essential.

Over the last several years the heat transfer in bubble column reactors has been the subject of many investigations²⁻⁶. On the other hand, only a little information is available on heat transport in airlift devices. The well known advantages of airlift reactors over the other types for a whole range of fermentations—bacterial, fungal, yeast, plant and animal tissue culture—are the stimulus for a better understanding of design, including heat transfer characteristics, of airlift systems.

This paper presents experimental results on gas-liquid heat transfer and gas holdup characteristics of concentric draught-tube type internal loop airlift vessels studied using model fluids for yeast, bacterial and fungal culture.

THEORY

Heat transfer from a heating surface immersed in a gas-liquid dispersion may be explained in terms of a mechanistic model which is conceptually similar to the surface renewal model used commonly in mass transfer studies. Thus, following Lewis et al.⁷, two contributions to heat transfer process can be envisaged: (i) Heat transfer by steady-state conduction in a stagnant liquid film adjacent to the heating surface; and (ii) heat transfer from the liquid film to bulk dispersion via 'packets' of liquid which are continually brought to the surface of the film from the bulk and are mixed again with the bulk fluid due to bubble induced agitation. The solution of the mathematical representation of those mechanisms was developed by Lewis et al.⁷, who, in relation to heat transfer in bubble columns, showed that the overall liquid heat transfer coefficient was given by

$$h = \left[\frac{\delta}{k_L} + \left(\frac{\pi\tau}{4k_L\rho_L C_P} \right)^{1/2} \right]^{-1} \quad (1)$$

where δ is the thickness of the stagnant liquid film on the heating surface and τ is some characteristic residence time of packets of fluid near the heating surface.

It has been established⁷ in bubble columns that heat transfer is dominated by the rate of heat removal by liquid packets and the film resistance only contributes a small part of the total heat transfer resistance. Because the nature of gas-liquid dispersion in bubble columns and airlift reactors is similar, the observation regarding the predominant transfer mechanism should apply also to airlift devices. In fact, the relatively higher liquid circulation attained in airlift reactors compared to bubble columns at otherwise identical conditions, would further ensure the dominance of transfer by liquid packets in the airlifts.

Hence, the first term of equation (1) can be neglected to give

$$h \propto \left(\frac{k_L\rho_L C_P}{\pi\tau} \right)^{1/2} \quad (2)$$

Practical use of equation (2) requires a knowledge of the contact time, τ . When the heat transfer surface is located in a chaotically turbulent field, as may be the case in bubble columns, the isotropic turbulence concept of Kolmogoroff may be used² to calculate the length (l) and the velocity (v) scales of microeddies. The latter have been regarded as being responsible for liquid renewal in the vicinity of the heating element. The contact time of fluid elements with the heating surface is then

$$\tau \approx l/v \quad (3)$$

This analysis of surface renewal heat transfer was propounded by Deckwer² for bubble columns. The later development of Lewis et al.⁷ disregarded isotropic turbulence as a source of surface renewal; instead, the authors⁷ combined the bulk liquid flow velocity as a function of radial position in the column with a characteristic length of the heat transfer surface to arrive at an estimate of the contact time. Airlift reactors produce high rates of liquid circulation and are, therefore, more turbulent than bubble columns. Hence, the surface renewal concept, so successfully used by Deckwer² in bubble columns, should apply to airlift systems.

0263-8762/89/\$05.00 + 0.00

© Institution of Chemical Engineers

From Kolmogoroff's turbulence theory, the length (l) and the velocity (v) scales of microeddies responsible for surface renewal are, respectively,

$$l = \left(\frac{v^3}{\epsilon} \right)^{1/4} \quad (4)$$

and

$$v = (l\epsilon)^{1/3} \quad (5)$$

Using equations (3) through (5) in equation (2) we obtain:

$$h \propto \left[\frac{k_L \rho_L C_P \epsilon^{1/2}}{v^{1/2}} \right]^{1/2} \quad (6)$$

The specific energy dissipation in airlift reactors is due predominantly to isothermal expansion of the sparged gas⁸, and it is given by:

$$\epsilon = g U_{sg} \quad (7)$$

Substitution of equation (7) in equation (6) leads to

$$h = \eta \left[\frac{k_L \rho_L C_P g^{1/2} U_{sg}^{1/2}}{v^{1/2}} \right]^{1/2} \quad (8)$$

Equation [8] relates the heat transfer coefficient to the principal operating parameter, the superficial gas velocity (U_{sg}).

EXPERIMENTAL

Experiments were carried out in concentric draught-tube airlifts with an outer tube 0.23 m in diameter and 1.22 m in height (Figure 1). Two different downcomers were used to give downcomer-to-riser area ratios of 0.242 and 0.452. The bottom of the column consisted of an inverted conical section with a cone angle of 45° (Figure 1). Twenty orifices of 1 mm diameter, located equidistant on a circle of 0.215 m diameter centered on the bottom of the cone, formed the gas sparger. This conical bottom geometry was developed for an aerobic fermentation process and it minimized the occurrence of dead spaces at the bottom of the reactor where biomass and substrate particles could be trapped⁹.

A temperature controller (YSI Model 74) with 1 kW heater and a temperature sensor (Figure 1) kept the

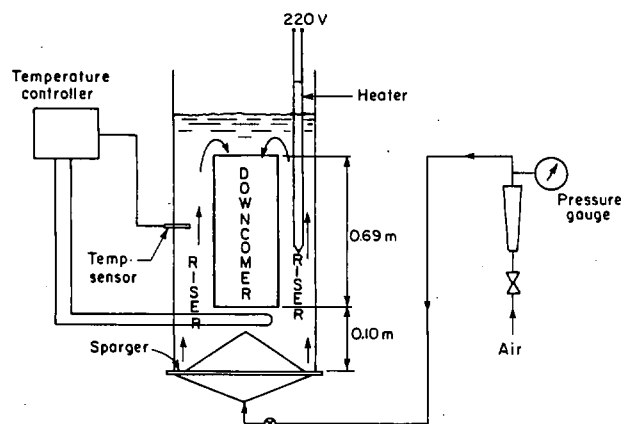


Figure 1. Airlift reactor. Dimensions in m, not to scale.

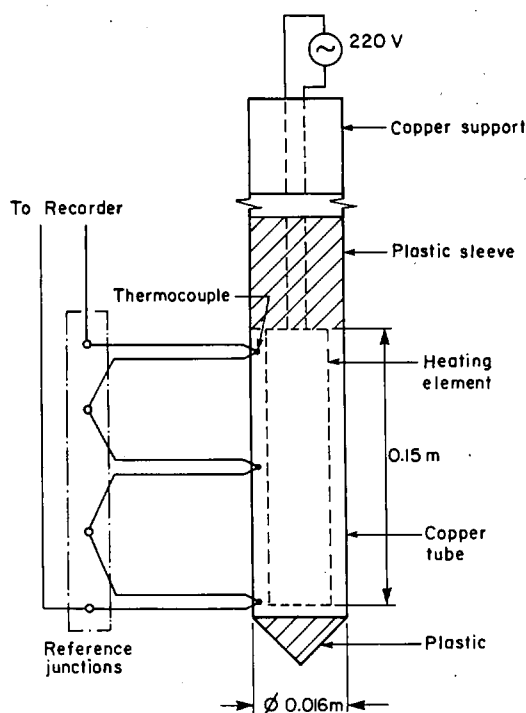


Figure 2. Heater assembly (schematic).

temperature of the bulk fluid constant ($\pm 1.0\%$). Within the instrument accuracy the bulk fluid temperature in the vessel was same everywhere for any controlled temperature value.

The heat load to reactors was provided by a heater (Figure 2) of the same basic design as used by Lewis et al.⁷ in bubble columns: A heating element (Chromalox C306, 30 W at 220 V) was placed in a copper tube. Three chromel-alumel thermocouples were positioned in holes drilled to 1.5 mm from the heating surface/liquid interface. The thermocouples were connected to provide an average heating surface temperature. The heater assembly was firmly supported in a vertical position in the riser or the downcomer of the reactors. Mains (220 V) power was used for heating and the power consumption was determined by watt/current meters.

For a range of air flow rates and heater power inputs, the heat transfer coefficients were calculated using the equation

$$h = \frac{W}{A_c \Delta T} \quad (9)$$

where ΔT was the steady state temperature difference between the heater and the bulk fluid. The effective area of the heater (A_c) was 0.0155 m².

Throughout either tap water or suspensions of Solka-Floc (James River Corporation, Grade KS 1016) cellulose fibres in aqueous salt solution (0.15 kmolm⁻³ NaCl) were used. The latter to simulate basic fungal fermentation media. The properties of Solka-Floc suspensions have been discussed in detail elsewhere¹⁰. The behaviour of these suspensions was visually the same as those of *Aspergillus niger* or *Chaetomium* broths.

Heat transfer coefficients and gas holdup (volume expansion method) were determined over a superficial

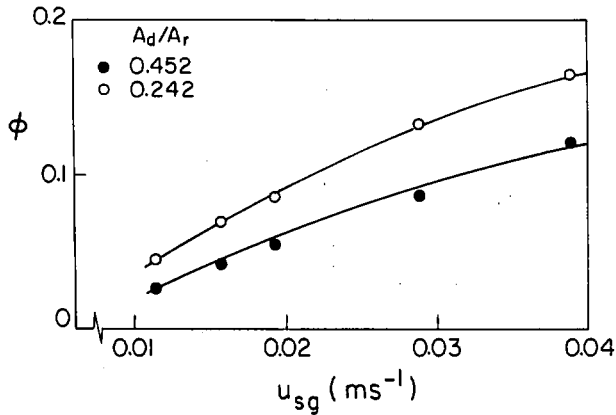


Figure 3. Variation of overall gas holdup with superficial gas velocity and with downcomer-to-riser cross-sectional area ratio in air-water.

air velocity range 0.01 to 0.04 ms^{-1} which corresponded to bubbly flow.

RESULTS AND DISCUSSION

The variation of gas holdup with superficial gas velocity and downcomer-to-riser cross-sectional area ratio is shown in Figure 3. The overall gas holdup declined with increasing A_d/A_r . This was because the enhanced liquid circulation with increasing A_d/A_r increased the bubble rise velocity. Increased liquid circulation with A_d/A_r in airlift vessels can be easily demonstrated from the work of Chisti et al.¹¹ For air-water the overall gas holdup could be correlated by:

$$\phi = 12.1 \left(1 + \frac{A_d}{A_r}\right)^{-2.8} U_{sg}^{1.1} \quad (10)$$

as shown in Figure 4.

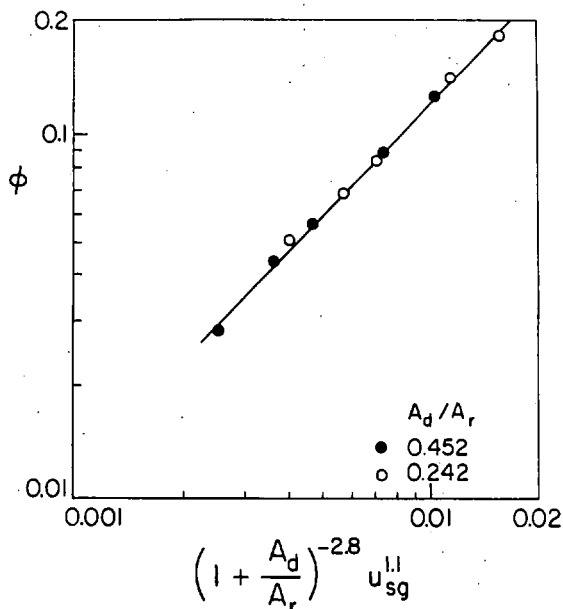


Figure 4. Overall gas holdup. Comparison of Equation (10) with experimental holdup in air-water.

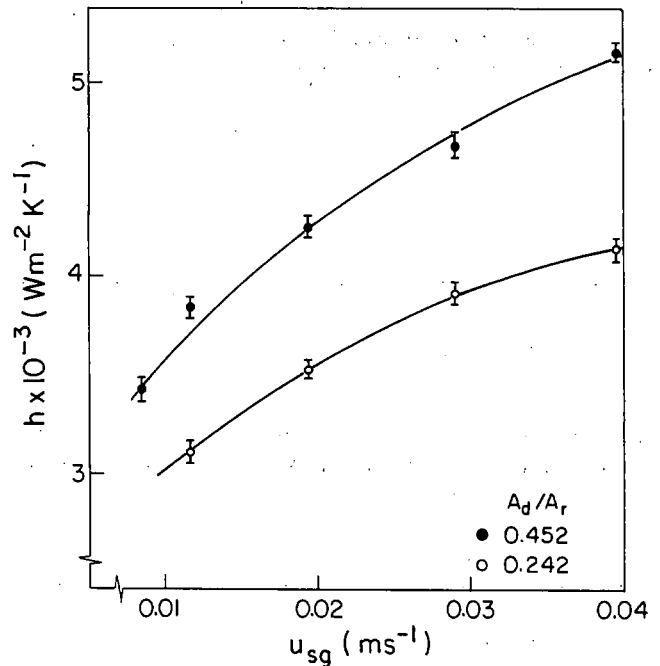


Figure 5. Heat transfer coefficient in riser: Influence of gas velocity and downcomer-to-riser cross-sectional area ratio.

The riser heat transfer coefficient calculated using equation (9) was in reality only a local value; the local heat transfer values find application in the practical problem of determining the most suitable location for heating and cooling surfaces in a reactor. We found no variation in heat transfer coefficient with either the axial or radial positioning of the heater in the risers. That is,

$$(h_{ave})_{Riser} = (h_{local})_{Riser} \quad (11)$$

As shown in Figure 5 the heat transfer coefficient in the riser increased with increasing A_d/A_r because of increased liquid velocity. Also, the strong positive effect of increasing gas velocity on riser heat transfer coefficient could be seen in Figure 5, and it was a result of improved turbulence which enhanced the rate of exchange of parcels of fluid between the heating surface and the bulk fluid. Addition of Solka-Floc solids to water led to a decline in the riser heat transfer coefficient as shown in Figure 6. The turbulence damping effect of solid particles may be a possible explanation for this phenomenon. A comparison of Figures 6(a) and (b) showed that the riser heat transfer coefficient in water was more sensitive to A_d/A_r ratio than the values obtained in suspensions. This was because only in water did the A_d/A_r ratio seem to have a strong influence on liquid circulation. For suspensions, suspension viscosity seemed to be the dominating influence, and the viscosity apparently did not vary much over the concentration range of solids.

Unlike in the riser, the downcomer heat transfer coefficient was found to depend on the axial position of the heater in the downcomer. As shown in Figure 7, the downcomer heat transfer coefficient decreased down the downcomer. There were several reasons for this: (i) downflow of liquid in the downcomer carried only the smallest gas bubbles down to the bottom of the downcomer, consequently there existed an axial distribution

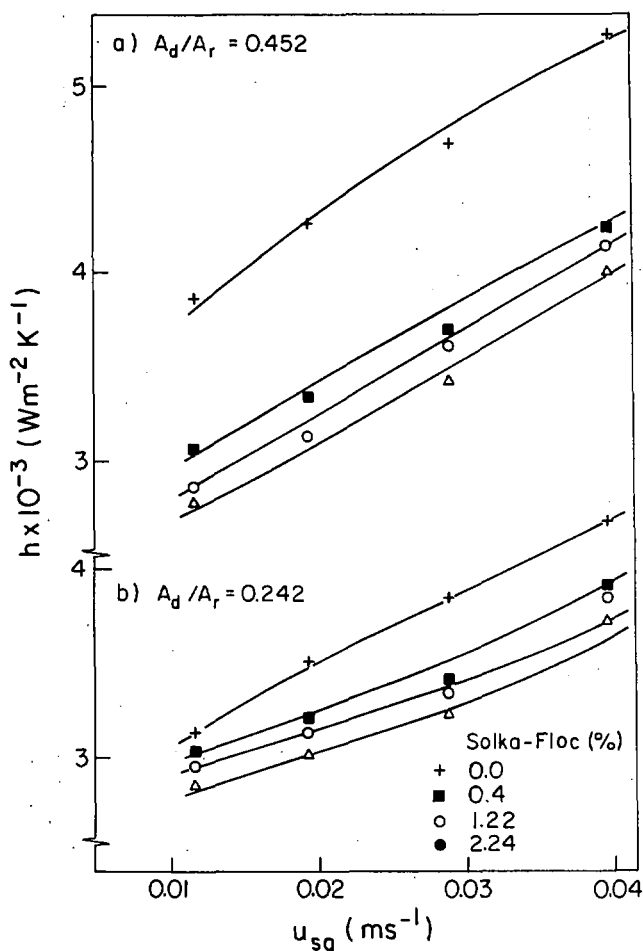


Figure 6. Heat transfer coefficient in riser: Influence of solids.

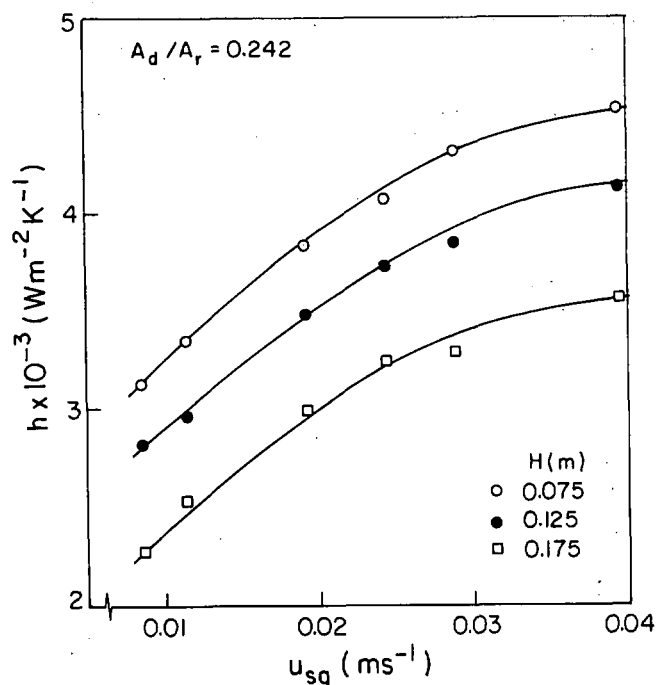


Figure 7. Downcomer heat transfer coefficient: Influence of heater location and riser gas velocity in air-water.

of gas holdup in the downcomer. In the upper regions of the downcomer the presence of large bubbles improved heat transfer, however, toward the bottom almost single phase flow existed and hence the lower heat transfer coefficient; (ii) the top zone of the downcomer, being closer to the entrance of the fluid in the downcomer, was additionally turbulent as a result of entrance effects and liquid flow became increasingly calm down the downcomer. Thus, the heat transfer coefficient declined down the downcomer.

In those cases in which the entire internal surface of the downcomer is used as the heat exchange surface, an average value of the heat transfer coefficient in the downcomer is the parameter of interest as opposed to some, local value. Thus, local values of heat transfer coefficient in the downcomer were graphically averaged with respect to height:

$$h_{\text{average}} = \frac{1}{H_2 - H_1} \int_{H_1}^{H_2} h_{\text{local}} dH \quad (12)$$

The variation of average heat transfer coefficient in the downcomer with gas velocity and A_d/A_r ratio is shown in Figure 8. Heat transfer coefficient increased as A_d/A_r declined—a trend different to that in the riser. The local heat transfer coefficient in the downcomer increased with increasing amounts of Solka-Floc solids (Figure 9), an effect opposite to that found in the riser. Clearly, the solid particles influenced the hydrodynamic conditions at the heating surface-liquid interface. Under highly turbulent conditions the addition of small quantities of solids may have a stirring effect near the heating surface; whereas the 'viscosity' influence may have been less pronounced than in the riser. This was reasonable because, firstly, the solid concentration did not vary much in Figure 9 and, secondly the downcomer liquid flow Reynolds numbers based on superficial liquid velocity were always higher by a factor of $(d_r/d_d) + 1$ (corresponded to 3.27 and 2.79 for the downcomers, respectively) than the value in the riser. Comparison of

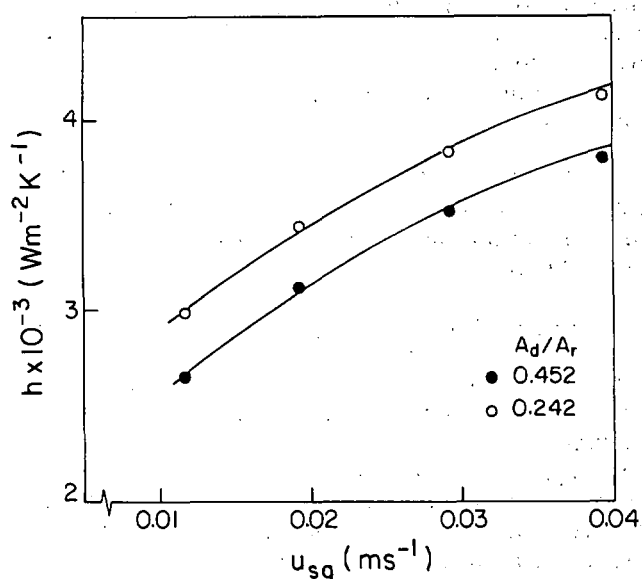


Figure 8. Average heat transfer coefficient in downcomer: Influence of downcomer-to-riser cross-sectional area ratio in air-water.

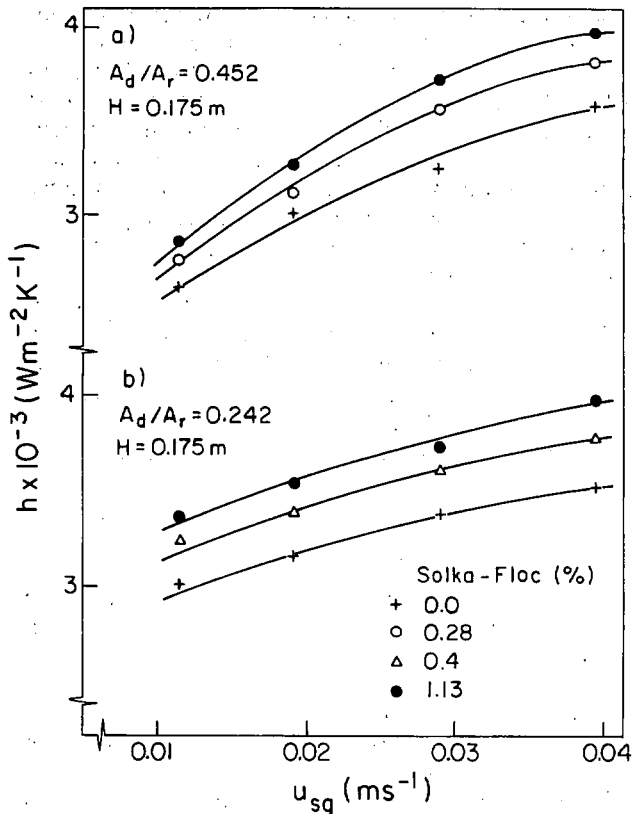


Figure 9. Local heat transfer coefficient in downcomer: Influence of solids and downcomer-to-riser cross-sectional area ratios.

Figures 9(a) and (b) showed a higher rate of increase of downcomer heat transfer coefficient with gas velocity in the vessel which had A_d/A_r of 0.242 (i.e. smaller downcomer, $d_d = 0.102$) relative to that for which A_d/A_r was 0.452. In both vessels, however, the limiting values of downcomer heat transfer obtained at U_{sg} of $\approx 0.04 \text{ ms}^{-1}$ were similar for any given fluid. The enhancement of downcomer heat transfer coefficients with increasing concentration of mycelial solids has also been observed by others^{12,13} for *Aspergillus niger* broths in external loop airlift reactors.

The overall, volume averaged, heat transfer coefficient defined as

$$h_T = (h_r A_r + h_d A_d) / A_T \quad (13)$$

is shown in Figure 10 for air-water where it is compared with the heat transfer correlation proposed by Deckwer² for bubble columns:

$$\frac{h_T}{\rho_L C_p U_{sg}} = 0.1 \left[\frac{\rho_L U_{sg}^3 (\mu_L C_p)^2}{\mu_L g (k_L)^2} \right]^{-1/4} \quad (14)$$

As shown in Figure 10, the airlift reactors had superior heat transfer performance than bubble columns.

Finally, as evidence for the basic form of our theoretical equation, we correlated the overall heat transfer coefficient with the superficial gas velocity; the best fit equation was found to be:

$$h_T = 1.334 \times 10^4 \left(1 + \frac{A_d}{A_r}\right)^{-0.7} U_{sg}^{0.275} \quad (15)$$

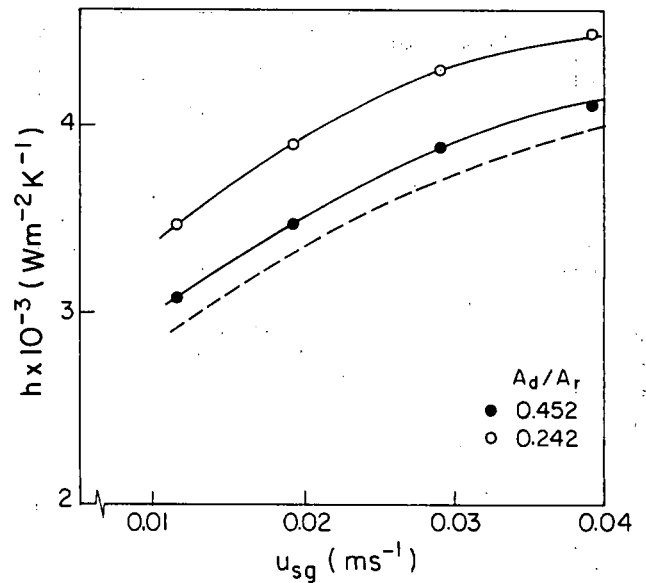


Figure 10. Overall heat transfer coefficient in airlift reactors in air-water. The dashed line for bubble columns is based on the correlation of Deckwer (2).

The theoretical equation (equation 8) predicted the exponent on U_{sg} to be 0.25 which was within 10% of the empirical value in equation (15). Similarly, the observed dependence of the overall heat transfer coefficient on the overall gas holdup was (Figure 11):

$$h_T \propto \phi^{0.241} \quad (16)$$

which was sensible because the overall holdup was approximately directly related to gas velocity (equation (10)) over the range examined.

The dependence of heat transfer coefficient on gas holdup suggests that the type of gas sparger may have some influence on heat transfer. A perforated plate sparger was used in this work; it is among the most common types of spargers in commercial practice. With other spargers, the exponent on gas velocity term in equation (15) may be somewhat different.

CONCLUSION

Airlift reactors were demonstrated to have better heat transfer characteristics than bubble columns. Experi-

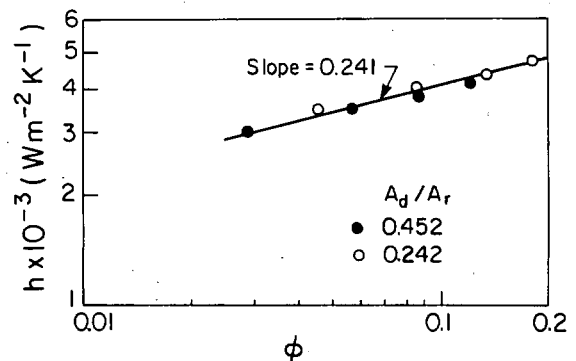


Figure 11. Overall heat transfer coefficient in airlifts in air-water vs. overall gas holdup.

mental evidence confirmed the theoretically predicted increase in heat transfer coefficient with increasing gas velocity in airlift devices. Additionally, the effect of mycelial type solids on heat transfer coefficient was shown to be either positive or negative, depending on the conditions of flow. Based on local heat transfer measurements the recommended location of heating surfaces in a concentric-tube airlift reactor was the riser. If the heating surface must be located in the downcomer, then the downcomer entrance would be the best possible location for it. In all cases heat transfer coefficients increased with increasing gas input.

NOMENCLATURE

A_d	Downcomer cross-sectional area (m^2)
A_e	Area for heat transfer (m^2)
A_r	Riser cross-sectional area (m^2)
A_T	Outer tube cross-sectional area (m^2)
C_p	Specific heat of liquid ($Jkg^{-1} K^{-1}$)
d_d	Downcomer diameter (m)
d_r	Outer tube diameter (m)
g	Gravitational acceleration (ms^{-2})
H	Depth of heater below liquid level (m)
$H_{1,2}$	Extremes of heater depth below liquid level (m)
h	Heat transfer coefficient ($Wm^{-2} K^{-1}$)
h_{ave}	Average heat transfer coefficient ($Wm^{-2} K^{-1}$)
h_{local}	Local heat transfer coefficient ($Wm^{-2} K^{-1}$)
h_T	Overall heat transfer coefficient for reactor ($Wm^{-2} K^{-1}$)
k_L	Thermal conductivity of liquid ($Wm^{-1} K^{-1}$)
ΔT	Temperature difference between heating surface and bulk liquid (K)
U_{sg}	Superficial gas velocity (ms^{-1})
v	Velocity of microeddy (ms^{-1})
W	Electrical power input to heater (W)

Greek Symbols

δ	Film thickness (m)
ϵ	Specific energy dissipation rate ($Jkg^{-1}s^{-1}$)
η	Proportionality constant in equation (8), dimensionless
l	Length of microeddy (m)
μ_L	Liquid viscosity (Pas)
ν	Kinematic viscosity ($m^2 s^{-1}$)
π	Pi
ρ_L	Liquid density ($kg m^{-3}$)
τ	Contact time (s)
ϕ	Overall gas holdup, dimensionless

REFERENCES

1. Kossen, N. W. F. quoted in Chisti, M. Y., 1989, *Airlift Bioreactors*, (Elsevier Applied Science, London).
2. Deckwer, W.-D., 1980, *Chem Eng Sci* 35: 1341.
3. Shah, Y. T., Kelkar, B. G., Godbole, S. P. and Deckwer, W.-D., 1982, *AIChE J.*, 28: 353.
4. Nishikawa, M., Kato, H. and Hashimoto, K., 1977, *Ind. Eng. Chem. Proc. Des. Dev.*, 16: 133.
5. Joshi, J. B., Sharma, M. M., Shah, Y. T., Singh, C. P. P., Ally, M. and Klinzing, G. E., 1980, *Chem. Eng Commun*, 6: 1.
6. Steiff, A. and Weinspach, P.-M., 1978, *Ger Chem. Eng.*, 1: 150.
7. Lewis, D. A., Field, R. W., Xavier, A. M. and Edwards, D., 1982, *Trans. IChem.E.* 60: 40.
8. Chisti, M. Y. and Moo-Young, M., 1987, *Chem Eng Commun*, 60: 195.
9. Moo-Young, M., Daugulis, A. J., Chahal, D. S. and Macdonald, D. G., 1979, *Process Biochem.* 14: 38.
10. Chisti, M. Y., Fujimoto, K. and Moo-Young, M., 1987, In Ho, C. S. and Oldshue, J. Y. (editors), *Biotechnology Processes: scale-up and mixing*, (American Institute of Chemical Engineers, New York), pp. 72.
11. Chisti, M. Y., Halard, B. and Moo-Young, M., 1988, *Chem Eng Sci*, 43: 451.
12. Blakebrough, N., Fatile, I. A., McManamey, W. J. and Walker, G., 1983, *Chem Eng Res Des* 61: 385.
13. Blakebrough, N., McManamey, W. J. and Tart, K. R., 1978, *Trans. IChemE*, 56: 127.

ACKNOWLEDGEMENT

This work was supported by a research grant from the Natural Science and Engineering Research Council of Canada.

ADDRESS

Correspondence concerning this paper should be addressed to Professor M. Moo-Young, Department of Chemical Engineering, University of Waterloo, Waterloo, Ontario, Canada N2L 3G1

The manuscript was communicated via our International Editor for Canada, Professor L. W. Shemilt. It was received 22 November 1988 and accepted for publication after revision 31 May 1989.